

# Optimum refractive-index profile of the graded-index polymer optical fiber, toward gigabit data links

Takaaki Ishigure, Eisuke Nihei, and Yasuhiro Koike

The optimum refractive-index distribution of the high-bandwidth graded-index polymer optical fiber (POF) was clarified for the first time by consideration of both modal and material dispersions. The ultimate bandwidth achieved by the POF is investigated by a quantitative estimation of the material dispersion as well as the modal dispersion. The results indicate that even if the refractive-index distribution is tightly controlled, the bandwidth of the graded-index POF is dominated by the material dispersion when the required bit rate becomes larger than a few gigabits per second. It is also confirmed that the material dispersion strongly depends on the matrix polymer and that the use of a fluorinated polymer whose material dispersion [ $-0.078$  ns/(nm km)] is lower than that of poly(methyl methacrylate) [ $-0.305$  ns/(nm km)] allows for a 10-Gb/s signal transmission.

*Key words:* Modal dispersion, material dispersion, graded index, polymer optical fiber (POF), high bandwidth, WKB method. © 1996 Optical Society of America

## 1. Introduction

Recent interests and developments in fiber-optic technology have permitted a high-speed multimedia network concept. However, the use of a single-mode glass fiber system is not necessarily suitable because of the requirement of precise handling and connection and thus the high cost in a broadband residential area network, i.e., asynchronous-transfer-mode-local area network, interconnection, and so on. In contrast, polymer optical fiber (POF), which has more than 500  $\mu\text{m}$  of core, is a promising candidate to solve such problems. Because all commercially available POF's have been of the step-index (SI) type, the modal dispersion limits the possible bit rate of POF links to less than 100 megabits per second (Mb/s). Therefore we proposed a large-core, low-loss, and high-bandwidth graded-index polymer optical fiber (GI POF),<sup>1,2</sup> and we confirmed that a 2.5-Gb/s signal transmission for a 100-m distance was possible with the GI POF.<sup>2,3</sup>

It is well known that the dispersion of the optical fiber is divided into three parts: modal dispersion, material dispersion, and waveguide dispersion. In the case of the SI POF, the modal dispersion is so large that the other two dispersions can be approximated to be almost zero. However, the quadratic refractive-index distribution in the GI POF can decrease the modal dispersion dramatically, and we succeeded in controlling the refractive-index profile of the GI POF to be an almost quadratic distribution by the interfacial-gel polymerization technique.<sup>2</sup> Therefore, in order to analyze the ultimate bandwidth characteristics of the GI POF, we clarify the optimum refractive-index profile, in which not only the modal dispersion but also the material dispersion is taken into account.

## 2. Experiment

### A. Sample Preparation

The material dispersion that is caused by the wavelength dependence of the refractive index was approximated by direct measurement of the refractive indices of polymer at several wavelengths. The samples of poly(methyl methacrylate) (PMMA) and poly(hexafluoro isopropyl 2-fluoroacrylate) (PHFIP 2-FA) bulks for the measurement were polymerized from their monomer. PHFIP 2-FA is one of the fluorinated polymers whose monomer unit contains

---

The authors are with the Faculty of Science and Technology, Keio University, 3-14-1, Hiyoshi, Kohoku-ku, Yokohama 223, Japan, and with the Kanagawa Academy of Science and Technology, 1-1-1, Fukuura, Kanazawa-ku, Yokohama 236, Japan.

Received 6 September 1995.

0003-6935/96/122048-06\$06.00/0

© 1996 Optical Society of America

only three carbon-hydrogen bonds. As dopants to control the refractive-index profile, benzyl benzoate (BEN) for PMMA and dibutyl phthalate (DBP) for PHFIP 2-FA were used. The dopant feed ratio to the monomer (monomer/dopant) was 5/1 (wt./wt.), which was the same ratio as that when the core of the GI POF was prepared. The monomer and dopant mixture with initiator and chain transfer agent was placed in a glass ampule with an inner diameter of 18 mm, and it was polymerized at 90 °C for 24 h. The method of polymerization of the polymer rod was described in detail in Refs. 4 and 5.

### B. Refractive Index

The refractive indices of the polymer bulks were measured by the use of Abbe's refractometer. As a way to measure the refractive indices at several wavelengths, an interference filter was inserted in Abbe's refractometer. Two or three measurements were made at each wavelength, and an average of those was employed. Usually, index measurements were fit to a three-term Sellmeier dispersion relation of the form<sup>6</sup>

$$n^2 - 1 = \sum_{i=1}^3 \frac{A_i \lambda^2}{\lambda^2 - l_i^2}, \quad (1)$$

where  $n$  is the refractive index of polymer sample,  $A_i$  is the oscillator strength,  $l_i$  is the oscillator wavelength, and  $\lambda$  is the wavelength of light.

## 3. Results and Discussion

### A. Refractive Index

Average refractive indices of the PMMA, BEN-doped PMMA, PHFIP 2-FA, and DBP-doped PHFIP 2-FA are summarized in Fig. 1 for different wavelengths,

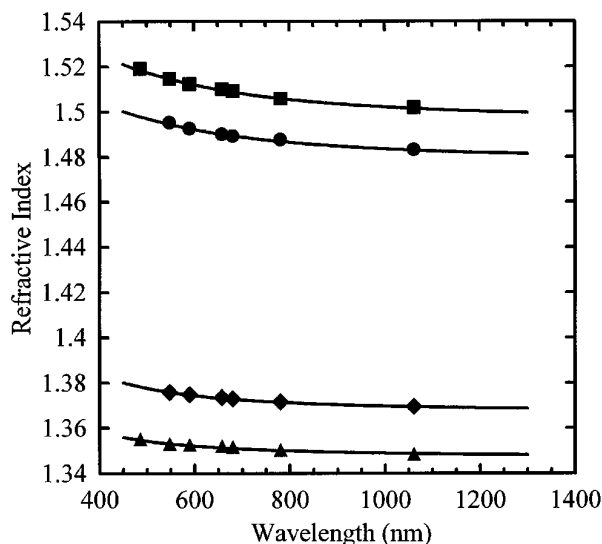


Fig. 1. Refractive-index dependence of the polymers on wavelength: ■, BEN-doped PMMA; ●, PMMA; ◆, DBP-doped PHFIP 2-FA; ▲, PHFIP 2-FA.

in which the solid curves are the best-fitted curves computed by a least-squares method. The coefficients resulting from the Sellmeier fitting are given in Table 1. It should be noted that the slopes of the refractive index versus wavelength curves indicate that the PHFIP 2-FA has a smaller dispersion of the refractive index with respect to wavelength than PMMA does.

### B. Material Dispersion

The material delay distortion  $D_{\text{mat}}$  for propagation of a pulse in the SI-type and the single-mode-types of optical fiber can be obtained from<sup>6</sup>

$$D_{\text{mat}} = -\left(\frac{\lambda \delta \lambda}{c}\right) \left(\frac{d^2 n}{d\lambda^2}\right) L, \quad (2)$$

where  $\sigma_1$  is the root-mean-square spectral width of the light source,  $\lambda$  is the wavelength of transmitted light,  $c$  is the velocity of light,  $d^2 n/d\lambda^2$  is the second-order dispersion, and  $L$  is length of the fiber.

Several measurements methods to investigate the material dispersion of the optical fiber have been already reported.<sup>7,8</sup> In addition, the material dispersion of the glass fiber could be measured directly by measurement of the delay time of the light pulse at several wavelengths through the fiber. However, this method cannot be applied to POF, because the higher attenuation of POF than glass optical fiber limits the transmission distance of the light pulses, and a high accuracy is required to detect the pulse delay time. Therefore dispersion measurements in the bulk samples of the polymer were adopted.

The material dispersions of PMMA, BEN-doped PMMA, PHFIP 2-FA, and DBP-doped PHFIP 2-FA are indicated in Fig. 2; they were calculated from the results of Sellmeier fitting, as shown Eqs. (1) and (2). The material dispersion of the silica obtained from Ref. 6 is also shown in curve (C) of Fig. 2. The material dispersion of the PMMA is larger than that of the silica from the visible to near infrared region. Furthermore, the signal wavelength for the PMMA-based GI POF is located in an optical window of transmission loss around a 650-nm wavelength. Therefore the material dispersion of the silica-based fiber at 1.3  $\mu\text{m}$  or 1.55  $\mu\text{m}$ , which are signal wavelengths, is much smaller than that of PMMA at a 650-nm wavelength.

At a wavelength of 650 nm, the material dispersion of PHFIP 2-FA is 0.136 ns/(nm km), whereas it is

Table 1. Coefficients of the Sellmeier Equation

Polymer	$A_1$	$l_1$	$A_2$	$l_2$	$A_3$	$l_3$
PMMA	0.4963	71.80	0.6965	117.4	0.3223	9237
PMMA-BEN	0.4855	104.3	0.7555	114.7	0.4252	49340
PHFIP 2-FA	0.4200	58.74	0.0461	87.85	0.3484	92.71
PHFIP 2-FA-DBP	0.2680	79.13	0.3513	83.81	0.2498	106.2

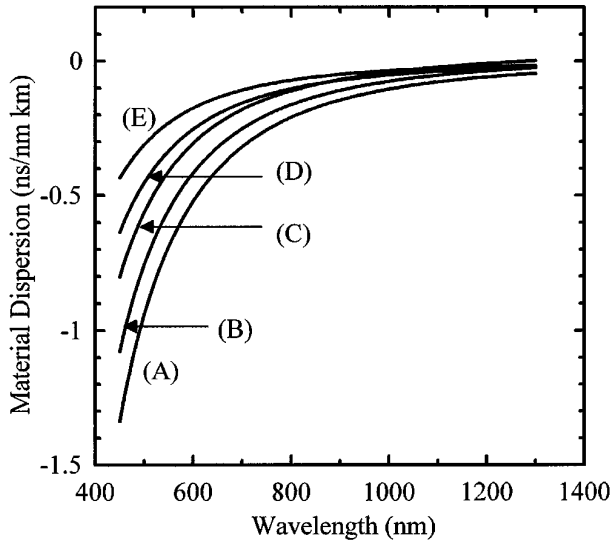


Fig. 2. Comparison of the material dispersion among PMMA, partially fluorinated polymer, and silica: (A), BEN-doped PMMA; (B), PMMA; (C), silica; (D), DBP-doped PHFIP 2-FA; (E), PHFIP 2-FA.

0.305 ns/(nm km) in the case of PMMA. In the case of the fluorinated polymer matrix, a small amount of an additive such as DBP or BEN, which has a large material dispersion, can increase the material dispersion of the doped polymer. Therefore a fluorinated dopant should be used for fluorinated polymer in order to keep the material dispersion lower.

### C. Refractive-index Profile Consideration

The material dispersion mentioned above indicates the pulse spread caused by the variance of the refractive index on the wavelength of light if a single-mode fiber or a SI fiber was fabricated by the polymer. In the case of the GI fiber, the effect of the refractive-index profile should be considered with the material dispersion.

The refractive-index profile was approximated by the conventional power law:

$$n(r) = n_1 \left[ 1 - \left( \frac{r}{a} \right)^\alpha \Delta \right], \quad (3)$$

$$\Delta = \frac{n_1^2 - n_2^2}{2n_1^2} \approx \frac{n_1 - n_2}{n_1}. \quad (4)$$

Here  $n_1$  and  $n_2$  are refractive indices at the center axis and the cladding of the fiber, respectively,  $a$  is the radius of the core,  $\alpha$  is the index exponent, and  $\Delta$  is the relative difference of the refractive index.

The output pulse width from the GI POF was calculated by the solution of the WKB method,<sup>9</sup> in which both modal and material dispersions were taken into account as shown in Eqs. (5)–(7). Here  $\sigma_{\text{intermodal}}$ ,  $\sigma_{\text{intramodal}}$ , and  $\sigma_{\text{total}}$  signify the root-mean-square pulse width caused by the modal dispersion,

the intramodal (material) dispersion, and both dispersions, respectively.

$$\sigma_{\text{intermodal}} = \frac{LN_1\Delta}{2c} \frac{\alpha}{\alpha + 1} \left( \frac{\alpha + 2}{3\alpha + 2} \right)^{1/2} \times \left[ C_1^2 + \frac{4C_1C_2\Delta(\alpha + 1)}{2\alpha + 1} + \frac{4\Delta^2C_2^2(2\alpha + 2)^2}{(5\alpha + 2)(3\alpha + 2)} \right]^{1/2}, \quad (5)$$

$$\sigma_{\text{intramodal}} = \frac{\sigma_s L}{\lambda} \left[ \left( -\lambda^2 \frac{d^2 n_1}{d\lambda^2} \right)^2 - 2\lambda^2 \frac{d^2 n_1}{d\lambda^2} (N_1 \Delta) \times C_1 \left( \frac{2\alpha}{2\alpha + 2} \right) + (N_1 \Delta)^2 \left( \frac{\alpha - 2 - \epsilon}{\alpha + 2} \right)^2 \times \left( \frac{2\alpha}{3\alpha + 2} \right)^2 \right]^{1/2}, \quad (6)$$

where

$$C_1 = \frac{\alpha - 2 - \epsilon}{\alpha + 2},$$

$$C_2 = \frac{3\alpha - 2 - 2\epsilon}{2(\alpha + 2)},$$

$$\epsilon = \frac{-2n_1 \lambda d\Delta}{N_1 \Delta d\lambda},$$

$$N_1 = n_1 - \lambda \frac{dn_1}{d\lambda}.$$

Here  $\sigma_s$  is the root-mean-square spectral width of the light source (in nanometers) and  $L$  is the fiber length.

$$\sigma_{\text{total}} = [(\sigma_{\text{intermodal}})^2 + (\sigma_{\text{intramodal}})^2]^{1/2}. \quad (7)$$

Figures 3 and 4 show the calculated  $\sigma_{\text{total}}$  versus index exponent  $\alpha$  for PMMA-based GI POF and PHFIP 2-FA-based GI POF, respectively. Here it was assumed that the fiber length and the spectral width of the light source (laser diode) were 100 m and 2 nm, respectively. Curves (A) in Figs. 3 and 4 indicate the pulse width calculated only by the modal dispersion; i.e., parameters  $\epsilon$  and  $\sigma_{\text{intramodal}}$  are zero and  $N_1$  equals  $n_1$  in Eqs. (5)–(7). In this case  $\sigma_{\text{total}}$  was minimized when  $\alpha$  equaled 1.97 in both PMMA-based and PHFIP 2-FA-based GI POF's. In contrast, when the material dispersion at the 650-nm wavelength was taken into account in Fig. 3, the total pulse width ( $\sigma_{\text{total}}$ ) becomes ten times larger, and the index exponent giving the smallest pulse width ( $\sigma_{\text{total}}$ ) is shifted to 2.33. It is also noteworthy that the effect of the material dispersion on the pulse width in PHFIP 2-FA-based GI POF in Fig. 4 is smaller than that in PMMA-based GI POF in Fig. 3.

From the results shown in Figs. 3 and 4, we

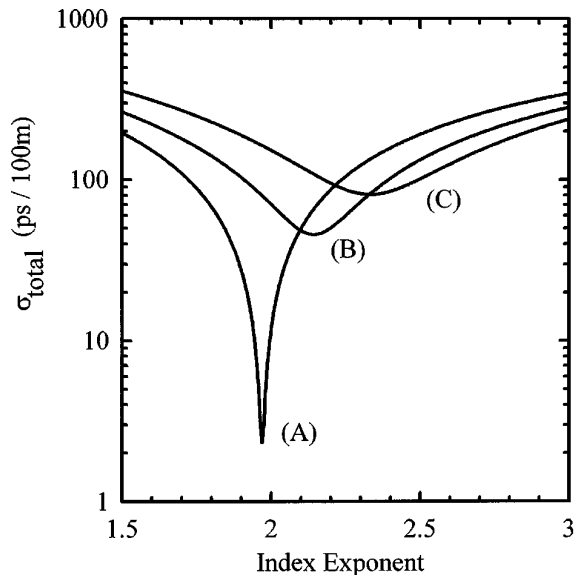


Fig. 3. Pulse width ( $\sigma_{total}$ ) versus index exponent of PMMA-based GI POF, assuming equal power in all modes and a light source having a rms spectral width of 2 nm: (A), only modal dispersion is considered; (B), both modal and material dispersions at a 780-nm wavelength are considered; (C), both modal and material dispersions at a 650-nm wavelength are considered.

estimated the possible bit rate in the GI POF link when the rms spectral width of the light source was assumed to be 2 nm. It was reported by Personick<sup>10,11</sup> that the power penalty of the receiver reaches 1 dB when the pulse width exceeds one fourth of the bit period [ $1/B$  (in seconds), where  $B$  is the bit rate

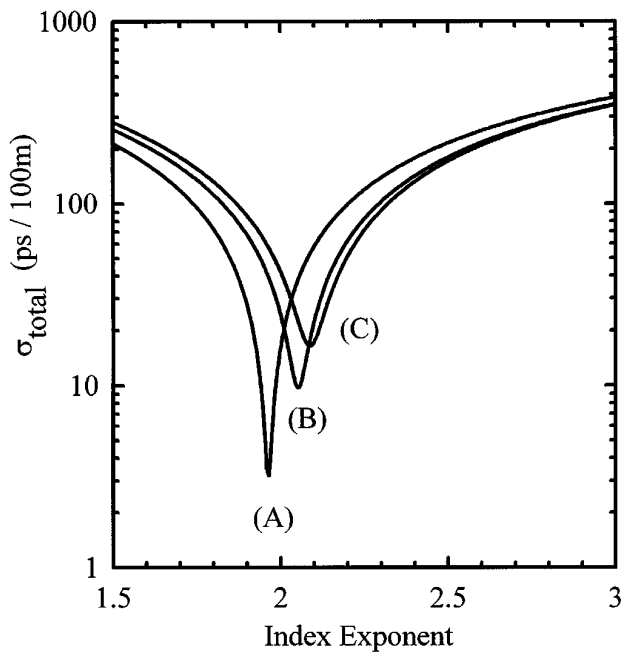


Fig. 4. Pulse width ( $\sigma_{total}$ ) versus index exponent of PHFIP 2-FA-based GI POF, assuming equal power in all modes and a light source having a rms spectral width of 2 nm: (A)–(C) are the same as in Fig. 3.

(bit/s)]. Therefore, possible bit rate  $B_p$  was defined by

$$B_p = \frac{1}{4\sigma_{total}} \quad (8)$$

The calculated possible bit rate in PMMA-based and PHFIP 2-FA-based GI POF links is shown in Fig. 5. The results indicate that the maximum bit rates of 25.7 Gb/s and 5.48 Gb/s can be achieved at a 780-nm wavelength in PHFIP 2-FA-based GI POF and PMMA-based GI POF links, respectively. In addition, the maximum bit rates at the 780-nm wavelength are higher than those at the 650-nm wavelength in both PHFIP 2-FA-based and PMMA-based GI POF links, because the material dispersion becomes smaller with the increase in wavelength of light, as shown in Fig. 2. The attenuation spectra of light transmission for both PMMA-based and PHFIP 2-FA-based GI POF's are shown in Fig. 6. As most carbon-hydrogen bondings in the PMMA-based GI POF are substituted for carbon-fluorine bondings in the PHFIP 2-FA-based POF, the absorption loss in the near-infrared-to-infrared region caused by the harmonic generation of carbon-hydrogen stretching vibration can be eliminated. Consequently, the total attenuation at the near-infrared region of the PHFIP 2-FA-based GI POF is lower than that of the PMMA-based GI POF as shown in Fig. 6. For instance, the attenuation of the PHFIP 2-FA-based GI POF at the 780-nm wavelength is 135 dB/km, whereas it is 840.5 dB/km in the PMMA-based GI POF. This low attenuation at the near-infrared region of the PHFIP 2-FA-based GI POF permits the use of an inexpensive laser diode as the light source

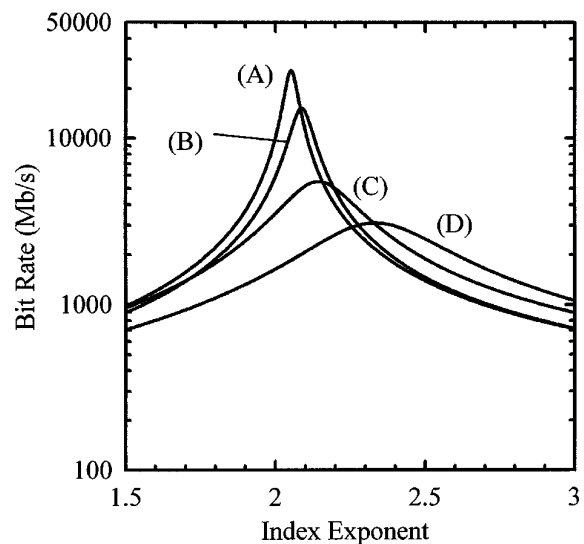


Fig. 5. Relation between the bit rate and index exponent of 100-m-length GI POF: (A), PHFIP 2-FA-based GI POF at a 780-nm wavelength; (B), PHFIP 2-FA-based GI POF at a 650-nm wavelength; (C), PMMA-based GI POF at a 780-nm wavelength; (D), PMMA-based GI POF at a 650-nm wavelength.

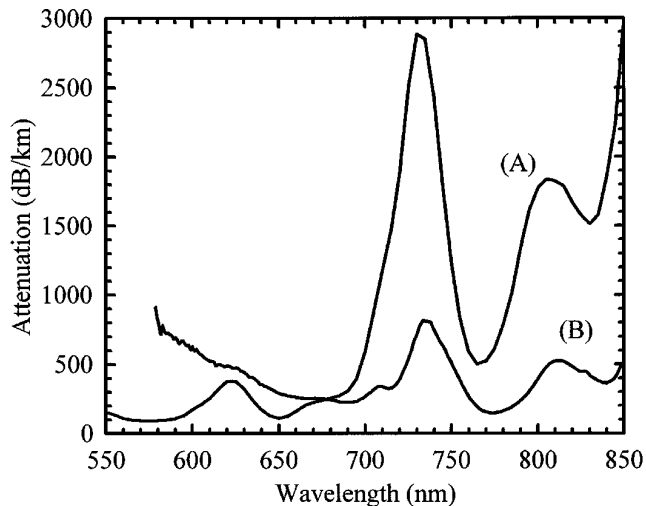


Fig. 6. Total attenuation spectra of the GI POF: (A), PMMA based; (B), PHFIP 2-FA based.

for a compact disc. Therefore the fluorinated polymer-based GI POF is advantageous because of the low attenuation at the near-infrared region and because of the low material dispersion.<sup>12</sup>

In the POF link, it has been proposed that an inexpensive LED can be utilized as the light source.<sup>13-15</sup> However, because the LED has a larger spectral width than the laser diode, the effect of the spectral width on the GI POF link by the LED should be investigated. The possible bit rate in a 100-m PMMA-based GI POF link is shown in Figs. 7 and 8, where the spectral widths of the light source are assumed to be 0, 1, 2, 5, and 20 nm. The wave-

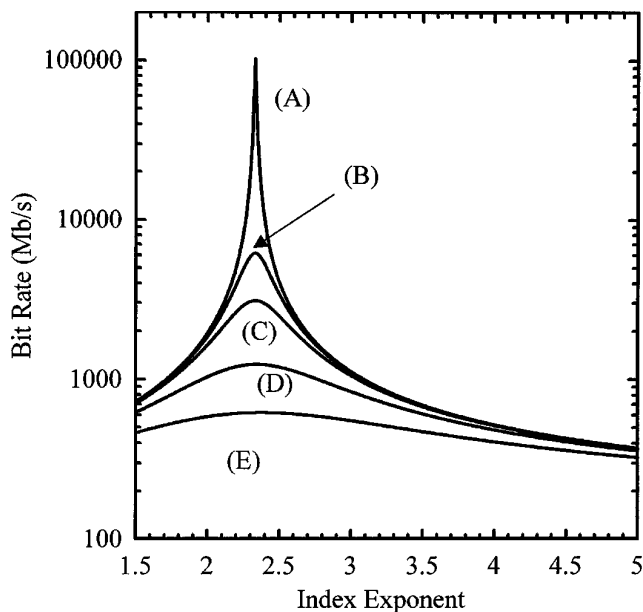


Fig. 7. Relation between the bit rate in the 100-m PMMA-based GI POF link and the index exponent at a 650-nm wavelength when the light source has a finite spectral width as follows: (A), 0 nm; (B), 1 nm; (C), 2 nm; (D), 5 nm; (E), 20 nm.

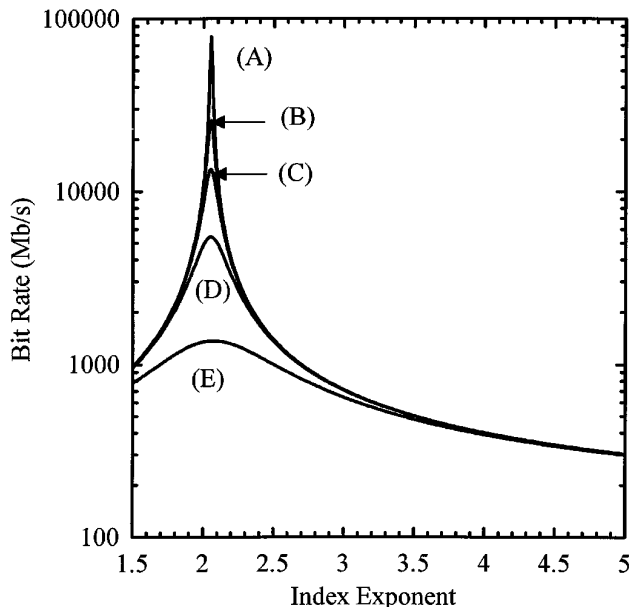


Fig. 8. Relationship between the bit rate in the 100-m PHFIP 2-FA-based GI POF link and the index exponent at a 780-nm wavelength when the light source has a finite spectral width as follows: (A), 0 nm; (B), 1 nm; (C), 2 nm; (D), 5 nm; (E), 20 nm.

lengths of the light sources in Figs. 7 and 8 are 650 nm and 780 nm, respectively.

In the case of the PMMA-based GI POF, the maximum bit rate dramatically decreases with an increase in the source spectral width, as shown in Fig. 7. When the source width is 20 nm, the bit rate becomes almost independent of the index exponent, as shown in curve (E) in Fig. 7. It was confirmed that it is impossible to cover more than 1 Gb/s of bit rate unless a light source with less than a 5-nm spectral width is used and the refractive-index profile is tightly controlled to the order of 2 to 3 of index exponent  $\alpha$ .

On the other hand, in the case of the PHFIP 2-FA-based GI POF, the low material dispersion makes it possible to transmit more than 1 Gb/s, even if the spectral width of the light source is more than 10 nm.

#### 4. Conclusion

The optimum refractive-index profile of the GI POF was clarified with both modal and material dispersions taken into account. The material dispersion seriously affects the bit rate performance of the GI POF link when the signal spectral width is larger than the order of nanometers. For a higher bit rate of more than 1 Gb/s in a 100-m POF link to be achieved, the source width should be less than 5 nm and the index profile of the PMMA-based GI POF should be controlled to the order of 2 to 3 of index exponent  $\alpha$ .

The PHFIP 2-FA-based GI POF can transmit a higher bit rate than the PMMA-based GI POF, even if the source width is as broad as 20 nm, because the

fluorinated polymer has low material dispersion. Furthermore, the low absorption loss of the PHFIP 2-FA-based GI POF at the near-infrared region permits the use of a longer wavelength in the POF link. It is concluded that the fluorinated polymer-based GI POF is superior to the PMMA-based GI POF in both the attenuation of light transmission and the total bit rate at the near-infrared region, where several inexpensive LED's and laser diodes exist.

## References

1. T. Ishigure, E. Nihei, and Y. Koike, "Graded-index polymer optical fiber for high-speed data communication," *Appl. Opt.* **33**, 4261–4266 (1994).
2. Y. Koike, T. Ishigure, and E. Nihei, "High-bandwidth graded-index polymer optical fiber," *IEEE J. Lightwave Technol.* **13**, 1475–1489 (1995).
3. T. Ishigure, E. Nihei, S. Yamazaki, K. Kobayashi, and Y. Koike, "2.5 Gb/s 100 m data transmission using graded index polymer optical fiber and high speed laser diode at 650-nm wavelength," *Electron. Lett.* **31**, 467–468 (1995).
4. Y. Koike, N. Tanio, and Y. Ohtsuka, "Light scattering and heterogeneities in low-loss poly(methyl methacrylate) glasses," *Macromolecules* **22**, 1367–1373 (1989).
5. Y. Koike, S. Matsuoka, and H. E. Bair, "Origin of excess light scattering in poly(methyl methacrylate) glasses," *Macromolecules* **25**, 4809–4815 (1992).
6. J. W. Fleming, "Material and mode dispersion in  $\text{GeO}_2 \cdot \text{B}_2\text{O}_3 \cdot \text{SiO}_2$  glasses," *J. Am. Ceram. Soc.* **59**, 503–507 (1976).
7. M. Horiguchi, Y. Ohmori, and T. Miya, "Evaluation of material dispersion using a nanosecond optical radiator," *Appl. Opt.* **18**, 2223–2228 (1979).
8. M. J. Heckert, "Development of chromatic dispersion measurement on multimode fiber using the relative time of flight measurement technique," *IEEE Photon. Technol. Lett.* **4**, 198–200 (1992).
9. R. Olshansky and D. B. Keck, "Pulse broadening in graded-index optical fibers," *Appl. Opt.* **15**, 483–491 (1976).
10. S. D. Personick, "Receiver design for digital fiber optic communication systems, I," *Bell Syst. Technol. J.* **52**, 843–874 (1973).
11. S. D. Personick, "Receiver design for digital fiber optic communication systems, II," *B.S.T.J.* **52**, 875–886 (1973).
12. T. Ishigure, E. Nihei, Y. Koike, C. E. Forbes, L. LaNieve, R. Straff, H. A. Deckers, "High-bandwidth graded-index polymer optical fiber for near infrared use," *IEEE Photon. Technol. Lett.* **7**, 403–405 (1995).
13. G. Garin, "High performance fiber optic links using low cost plastic fiber," presented at the Plastic Optical Fibers and Applications Conference, Paris, France, 22–23 June 1992.
14. K. Fukuda and T. Iwakami, "High-speed and long-distance POF transmission systems based on LED transmitters," presented at the Plastic Optical Fibers and Applications Conference, The Hague, The Netherlands, 28–29 June 1993.
15. A. Nakamura, N. Horie, Y. Kitagawa, T. Tanaka, J. Takagi, T. Yamashita, K. Veda, and H. Naito, "Highly efficient power coupling between a LED and a plastic optical fiber," presented at the Plastic Optical Fibers and Applications Conference, Yokohama, Japan, 26–28 October 1994.